# Role of vector mesons in high-$Q^2$ lepton-nucleon scattering

W. Melnitchouk and A. W. Thomas
*Department of Physics and Mathematical Physics, University of Adelaide, Box 498 G.P.O., Adelaide, 5001 Australia*
(Received 14 December 1992)

The possible role played by vector mesons in inclusive deep-inelastic lepton-nucleon scattering is investigated. In the context of the convolution model, we calculate self-consistently the scaling contribution to the nucleon structure function using the formalism of time-ordered perturbation theory in the infinite momentum frame. Our results indicate potentially significant effects only when the vector-meson–nucleon form factor is very hard. Agreement with the experimental antiquark distributions, however, requires relatively soft form factors for the $\pi N$, $\rho N$, and $\omega N$ vertices.

PACS number(s): 13.60.Hb, 12.38.Lg, 12.40.Aa

## I. INTRODUCTION

In the context of meson-exchange models of the $NN$ force in nuclear physics, it has long been realized that vector mesons play a vital role [1,2]. For example, the isovector $\rho$ meson is needed to provide sufficient cancellation of the tensor force generated by $\pi$ meson exchange, which would otherwise be too large. On the other hand, the isoscalar $\omega$ meson, through its large vector coupling, is responsible for the short range $NN$ repulsive force, and also provides most of the spin-orbit interaction. Traditionally it has been necessary to use hard vector-meson–nucleon form factors in order to fit the $NN$ phase shifts [2]. However, alternative approaches have recently been developed in which the $NN$ data can be fitted with quite soft form factors [3,4].

From another direction, the vector-meson dominance model of the elastic electromagnetic nucleon form factors, in which an isovector photon couples to the nucleon via a $\rho$ meson, provides a natural explanation of the dipole $Q^2$ behavior of the $\gamma NN$ vertex function. Recent analyses [3] have shown that a $\rho NN$ vertex parameterized by a soft monopole form factor ($\Lambda_1 \sim 800$ MeV) provides a good description of the $Q^2$ dependence of the Dirac and Pauli form factors. The effect of vector mesons upon nucleon electromagnetic form factors has also been explored [5] in the cloudy bag model [6], and in various soliton models [7].

In this paper we investigate the possible role played by vector mesons in high-$Q^2$ inelastic inclusive scattering of leptons from nucleons, in the context of the so-called convolution model, in which the deep-inelastic process is described in terms of both quark and explicit meson-baryon degrees of freedom. More specifically, the scaling property of the meson- and baryon-exchange contributions to the inclusive cross section allows us to probe the extended mesonic structure of nucleons.

Quite naturally the pion, being by far the lightest meson, was the first meson whose contributions to the nucleon structure function were investigated [8]. It was later noticed [9] that the pion cloud could be responsible for generating an asymmetry between the $\bar{u}$- and $\bar{d}$-quark content of the proton sea, through the preferred proton dissociation into a neutron and $\pi^+$. Furthermore, deep-inelastic scattering (DIS) data on the momentum fractions carried by antiquarks were used to obtain an upper limit on this nonperturbative pionic component [9,10]. An enhancement of $\bar{d}$ over $\bar{u}$ resulting from this process was also postulated as one explanation for the slope of the rapidity distribution in $p$-nucleus Drell-Yan production [11]. More recently it has been hypothesized that this asymmetry could account for some of the apparent discrepancy between the naive parton model prediction for the Gottfried sum rule [12] and its recently determined experimental value [13], and indeed this has resulted in the greater attention that the convolution model of lepton-nucleon scattering has received [14–21].

In a model in which the nucleon has internal meson and baryon degrees of freedom, the physical nucleon state in an infinite momentum frame can be expanded (in the one-meson approximation) in a series involving bare nucleon and two-particle meson-baryon states:

$$|N\rangle_{\rm phys}=\sqrt{Z}\left\{|N\rangle_{\rm bare}+\sum_{MB}\int dy\, d^2\mathbf{k}_T\, g_{0_{MBN}}\phi_{MB}(y,\mathbf{k}_T)|M(y,\mathbf{k}_T);B(1-y,-\mathbf{k}_T)\rangle\right\} . \tag{1}$$

Here, $\phi_{MB}(y,\mathbf{k}_T)$ is the probability amplitude for the physical nucleon to be in a state consisting of a meson $M$ and baryon $B$, having transverse momenta $\mathbf{k}_T$ and $-\mathbf{k}_T$, and carrying longitudinal momentum fractions $y$ and $1-y$, respectively. $Z$ is the bare nucleon probability. Although we work in the one-meson approximation, we will include higher-order vertex corrections to the bare coupling constants $g_{0_{MBN}}$. Illustrated in Fig. 1 is the deep-inelastic scattering of the virtual photon from the two-particle state $|M;B\rangle$. In Fig. 1(a) the photon interacts with a quark or antiquark inside the exchanged meson, while in Fig. 1(b) the scattering is from a quark in the baryon component of the physical nucleon.

According to Eq. (1), the probability to find a meson inside a nucleon with momentum fraction $y(=k\cdot q/p\cdot q)$ is (to leading order in the coupling constant)

 

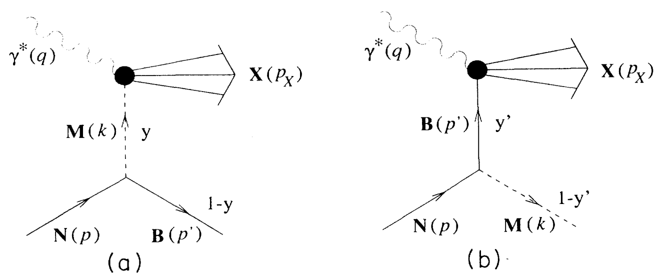


FIG. 1. Deep-inelastic scattering from the virtual (a) meson and (b) baryon components of a physical nucleon.

$f_{MB}(y) \equiv Z g^2_{0_{MBN}} \int d^2\mathbf{k}_T |\phi_{MB}(y,\mathbf{k}_T)|^2$. This must also be the probability to find a baryon inside a nucleon with momentum fraction $1-y$. The baryon distribution function $f_{BM}(y')$, where $y'=p'\cdot q/p\cdot q$, is probed directly through the process in Fig. 1(b), and should be related to the meson distribution function by

$$f_{MB}(y)=f_{BM}(1-y) \tag{2}$$

for all $y$, if the above interpretation is valid. We also demand equal numbers of mesons emitted by the nucleon, $\langle n \rangle_{MB} = \int_0^1 dy\, f_{MB}(y)$, and virtual baryons accompanying them, $\langle n \rangle_{BM} = \int_0^1 dy' f_{BM}(y')$:

$$\langle n \rangle_{MB} = \langle n \rangle_{BM} \; . \tag{3}$$

This is just a statement of charge conservation. Momentum conservation imposes the further requirement that

$$\langle y \rangle_{MB} + \langle y \rangle_{BM} = \langle n \rangle_{MB} \tag{4}$$

where $\langle y \rangle_{MB} = \int_0^1 dy\, y\, f_{MB}(y)$ and $\langle y \rangle_{BM} = \int_0^1 dy' y' f_{BM}(y')$ are the average momentum fractions carried by meson $M$ and the virtual baryon $B$, respectively. Equations (3) and (4), and in fact similar relations for all higher moments of $f(y)$, follow automatically from Eq. (2).

In what follows we shall explicitly evaluate the functions $f_{MB}$ and $f_{BM}$, and examine the conditions under which Eq. (2) is satisfied. The results will be used to calculate the contributions to the nucleon structure function from the extended mesonic structure of the nucleon, which are expressed as convolutions of the functions $f(y)$ with the structure functions of the struck meson or baryon:

$$\delta^{(MB)}F_{2N}(x) = \int_x^1 dy\, f_{MB}(y) F_{2M}(x/y) \; , \tag{5}$$

$$\delta^{(BM)}F_{2N}(x) = \int_x^1 dy' f_{BM}(y') F_{2B}(x/y') \; , \tag{6}$$

with $x=-q^2/2p\cdot q$ being the Bjorken variable. Note that Eqs. (5) and (6) are correct when physical (renormalized) meson-baryon coupling constants are used in the functions $f_{MB}$ and $f_{BM}$ (see Sec. IV for details). By comparing against the experimental structure functions, we will ultimately test the reliability of the expansion in Eq. (1), and in particular the relative importance of the states involving vector mesons compared with the pion states.

## II. THE PION-NUCLEON CONTRIBUTION

### A. Covariant formulation

Traditionally the effects upon $F_{2N}(x)$ of the $\pi$ meson cloud have been studied most intensely. The distribution function of a virtual pion accompanied by a recoiling nucleon has been calculated in a covariant framework [8,9] as

$$f_{\pi N}(y) = \frac{3g^2_{\pi NN}}{16\pi^2} y \int_{-\infty}^{t^N_{\max}} dt \frac{(-t)\mathcal{F}^2_{\pi N}(t)}{(t-m^2_\pi)^2} \; . \tag{7}$$

Here, $t \equiv k^2 = t^N_{\max} - k^2_T/(1-y)$ is the four-momentum squared of the virtual pion, with a kinematic maximum given by $t^N_{\max} = -m^2_N y^2/(1-y)$, and $k^2_T$ is the pion transverse momentum squared. In a covariant formulation the form factor $\mathcal{F}_{\pi N}$ parametrizing the $\pi NN$ vertex, at which only the pion is off-mass-shell, can only depend on $t$.

Contributions from processes in which the virtual nucleon (accompanied by a recoiling pion) is struck have been calculated by several authors [18,20,22], although not all agree. Partly because there is less phenomenological experience with so-called sideways form factors (where the nucleon, rather than the pion, is off-mass-shell), some early work [23,15,17] simply defined $f_{N\pi}(y')$ through Eq. (2). However, this is unsatisfactory from a theoretical point of view, and ideally we would like to verify explicitly that the functions $f_{\pi N}$ and $f_{N\pi}$ satisfy Eq. (2).

Clearly the treatment of deep-inelastic scattering from an interacting nucleon is considerably more involved than that from a real nucleon, which is described by the usual hadronic tensor

$$W^{\mu\nu}_N(p,q) = \tilde{g}^{\mu\nu} W_{1N}(p,q) + \tilde{p}^\mu \tilde{p}^\nu W_{2N}(p,q) \; , \tag{8}$$

where $\tilde{g}^{\mu\nu} = -g^{\mu\nu} + q^\mu q^\nu/q^2$ and $\tilde{p}^\mu = p^\mu - q^\mu p\cdot q/q^2$. The hadronic vertex factor for the diagram of Fig. 1(b) in this case will be

$$\mathrm{Tr}[(\not{p}+m_N) i\gamma_5 (\not{p}'+m_N) \hat{W}^{\mu\nu}_N(p',q)(\not{p}'+m_N) i\gamma_5] \; , \tag{9}$$

where $\hat{W}^{\mu\nu}_N(p',q)$ is a matrix in Dirac space representing the hadronic tensor for an interacting nucleon, and is related to the hadronic tensor for real nucleons by [24]

$$W^{\mu\nu}_N(p,q) = \tfrac{1}{2}\mathrm{Tr}[(\not{p}+m_N)\hat{W}^{\mu\nu}_N(p,q)] \; . \tag{10}$$

If the struck nucleon is treated as an elementary fermion [25] the relevant operator in $\hat{W}^{\mu\nu}_N(p',q)$ is $\not{q}/2p'\cdot q$, which leads to [22]

$$f_{N\pi}(y') = \frac{3g^2_{\pi NN}}{16\pi^2} y' \int_{-\infty}^{t'^\pi_{\max}} dt' \left[ -m^2_\pi - \frac{1-y'}{y'}(t'-m^2_N) \right] \times \frac{\mathcal{F}^2_{N\pi}(t')}{(t'-m^2_N)^2} \; , \tag{11}$$

where $t' \equiv p'^2 = t'^\pi_{\max} - p'^2_T(1-y')$ is the four-momentum squared of the virtual nucleon, with the upper limit now given by $t'^\pi_{\max} = m^2_N y' - m^2_\pi y'/(1-y')$, and $p'^2_T$ denotes the nucleon's transverse momentum squared. Apart from the form factors, Eqs. (7) and (11) are clearly related by an interchange $y'\leftrightarrow 1-y$.

Note that choosing a different operator form for $\hat{W}_N^{\mu\nu}$ may lead to unphysical results. For example, with an operator involving $I$ rather than $\not{q}$ the trace factor in Eq. (11) is proportional to $-m_\pi^2$. Problems also arise for the emission of scalar or vector mesons [26]. A full investigation of the off-mass-shell effects in deep-inelastic structure functions of composite objects will be the subject of a future publication [27].

The large-$t'$ suppression for the $N\pi N$ vertex is introduced by the form factor $\mathcal{F}_{N\pi}$, which is usually parametrized by a monopole or dipole function

$$\mathcal{F}_{N\pi}(t')=\left[\frac{\Lambda_{N\pi}^2-m_N^2}{\Lambda_{N\pi}^2-t'}\right]^n$$

for $n=1$ and 2, respectively. However, to satisfy Eq. (3), the cutoff parameter $\Lambda_{N\pi}$ will in general have to be different from the cutoff $\Lambda_{\pi N}$ regulating the $\pi NN$ vertex form factor in Eq. (7):

$$\mathcal{F}_{\pi N}(t)=\left[\frac{\Lambda_{\pi N}^2-m_\pi^2}{\Lambda_{\pi N}^2-t}\right]^n .$$

In general a different $\Lambda_{\pi N}$ would be required to satisfy Eq. (4), and it would not be possible to guarantee Eq. (2).

Another important assumption in the covariant convolution model is that the dependence of the virtual meson and baryon structure functions in Eqs. (5) and (6) on the invariant mass squared is negligible. The argument usually made is that the vertex form factor suppresses contributions from the far off-mass-shell configurations (i.e., for $|t|\gtrsim 10m_N^2$ [17]). However, in this approach even the identification of the off-shell structure functions themselves is not very clear. Some suggestions about how to relate the off-shell functions to the on-shell ones were made [28] in the context of DIS from nuclei, although these were more *ad hoc* prescriptions rather than theoretical derivations. Attempts to simplify this situation were made in Ref. [29], where it was proposed that the instant form of dynamics, where only on-mass-shell particles are encountered, be used to calculate the nuclear structure functions. Along similar lines was the light-front approach of Berger *et al.* [23]. Actually these two techniques are the same if one works in the infinite momentum frame. The instant form of dynamics was previously used by Güttner *et al.* [30] in the calculation of the function $f_{\pi N}(y)$ for the case of pion electroproduction, and more recently by Zoller [20] in the DIS of charged leptons from nucleons.

### B. Infinite momentum frame states

An alternative to the use of covariant Feynman diagrams, in the form of "old-fashioned" time-ordered perturbation theory in the infinite momentum frame (IMF), was proposed some time ago by Weinberg [31] for scalar particles. This was later extended by Drell, Levy, and Yan [32] to the $\pi N$ system in deep-inelastic scattering. The main virtues of this approach are that off-mass-shell ambiguities in the structure functions of virtual particles can be avoided, and that the meson and baryon distribution functions can be shown to satisfy Eq. (2) exactly.

In the time-ordered theory the analogue of Fig. 1(a) will now involve two diagrams in which the $\pi$ moves forwards and backwards in time, Fig. 2. However, in a frame of reference where the target nucleon is moving fast along the $z$ direction with longitudinal momentum $p_L(\rightarrow\infty)$, only that diagram involving a forward moving pion gives a nonzero contribution. In the IMF the target nucleon has energy

$$p_0=p_L+\frac{m_N^2}{2p_L}+O\left[\frac{1}{p_L^2}\right] .$$

Following Weinberg [31] we write the pion three-momentum as

$$\mathbf{k}=y\mathbf{p}+\mathbf{k}_T ,$$

where $\mathbf{k}_T\cdot\mathbf{p}=0$, and conservation of momentum demands that the recoil nucleon momentum be

$$\mathbf{p}'=(1-y)\mathbf{p}-\mathbf{k}_T .$$

Since all particles are on their mass shells the energies of the intermediate $\pi$ and $N$ must be

$$k_0=|y|p_L+\frac{k_T^2+m_\pi^2}{2|y|p_L}+O\left[\frac{1}{p_L^2}\right] ,$$

$$p_0'=|1-y|p_L+\frac{k_T^2+m_N^2}{2|1-y|p_L}+O\left[\frac{1}{p_L^2}\right] .$$

For forward moving particles [Fig. 2(a)] $y$ and $1-y$ are positive, and according to the rules of the time-ordered perturbation theory the energy denominator appearing in the calculation of $f_{\pi N}(y)$ is $(p_0-p_0'-k_0)$

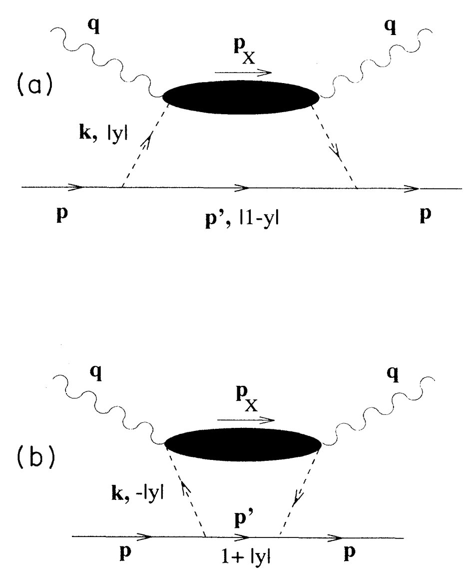


FIG. 2. Time-ordered diagrams for pions moving (a) forwards and (b) backwards in time. Time is increasing from left to right.

$=(m_N^2-s_{\pi N})/2p_L$, where

$$s_{\pi N}=s_{\pi N}(k_T^2,y)=(p_0'+k_0)^2-(\mathbf{p}'+\mathbf{k})^2 =\frac{k_T^2+m_\pi^2}{y}+\frac{k_T^2+m_N^2}{1-y} \tag{12}$$

is the center-of-mass energy squared of the intermediate $\pi N$ state. Changing the variables of integration from $d^3\mathbf{k}$ to $dy$ and $dk_T^2$, all powers of $p_L$ are seen to cancel when combined with the appropriate vertex factors $(2p_0')^{-1}$ and $(2k_0)^{-2}$. However, for a backward moving pion [Fig. 2(b)] $y$ is negative, and the energy denominator becomes $(p_0-p_0'-k_0)=2yp_L+O(1/p_L)$. Therefore in the $p_L\to\infty$ limit this time ordering does not contribute, and the result of Eq. (7) is reproduced, form factor aside.

For an interacting nucleon with $\pi$ recoil, Fig. 3, the kinematics are similar to the above, namely the nucleon and pion move with three-momenta

$$\mathbf{p}'=y'\mathbf{p}-\mathbf{k}_T\ ,$$

$$\mathbf{k}=(1-y')\mathbf{p}+\mathbf{k}_T\ ,$$

and have energies

$$p_0'=|y'|p_L+\frac{k_T^2+m_N^2}{2|y'|p_L}+O\left[\frac{1}{p_L^2}\right]\ ,$$

$$k_0=|1-y'|p_L+\frac{k_T^2+m_\pi^2}{2|1-y'|p_L}+O\left[\frac{1}{p_L^2}\right]\ ,$$

respectively. The general structure of the tensor describing a nonelementary interacting nucleon can be written as

$$\hat{W}_N^{\mu\nu}(p,q)=\tilde{g}^{\mu\nu}(\hat{W}_0+\not{p}\hat{W}_1+\not{q}\hat{W}_2)+\cdots\ , \tag{13}$$

where we have omitted terms proportional only to $p^{\mu,\nu}$ and $q^{\mu,\nu}$. The functions $\hat{W}_{0,1,2}$ are related to the on-mass-shell structure function $W_{1N}$ by Eq. (10):

$$W_{1N}(p,q)=2(m_N\hat{W}_0+m_N^2\hat{W}_1+p\cdot q\hat{W}_2)\ . \tag{14}$$

Then direct evaluation of the trace in Eq. (9) gives

$$4(2p\cdot p'-2m_N^2)[\tilde{g}^{\mu\nu}(m_N\hat{W}_0+m_N^2\hat{W}_1+p'\cdot q\hat{W}_2)+\cdots]$$
$$=2(2p\cdot p'-2m_N^2)\tilde{g}^{\mu\nu}W_{1N}(p',q)+\cdots$$

where now the exact on-shell nucleon structure function appears, and there is no off-shell ambiguity.

For a backward moving nucleon [Fig. 3(b)] $y'$ is negative, and $2p\cdot p'-2m_N^2=-4y'p_L^2+O(1/p_L)$, so that the numerator becomes large in the $p_L\to\infty$ limit. Technically this is due to the "badness" of the operator $\gamma_5$, which mixes upper and lower components of the nucleon spinors. The energy denominator here is $(p_0-p_0'-k_0)=2y'p_L+O(1/p_L)$, and when squared and combined with the $1/p_L^2$ from the integration and vertex factors, the contribution from this diagram vanishes when $p_L$ is infinite.

Therefore we need only evaluate the diagram with the forward moving nucleon, Fig. 3(a), which gives the result of Eq. (11):

$$f_{N\pi}(y')=\frac{3g_{\pi NN}^2}{16\pi^2}\int_0^\infty dk_T^2\left[\frac{k_T^2+(1-y')^2m_N^2}{y'}\right] \times\frac{\mathcal{F}_{N\pi}^2(k_T^2,y')}{y'(1-y')(m_N^2-s_{N\pi})^2}\ , \tag{15}$$

with $s_{N\pi}(k_T^2,y')=s_{\pi N}(k_T^2,1-y')$, except that the form factor is now unknown. It is quite natural to choose the form factor to be a function of the center-of-mass energy squared of the $\pi N$ system, $s_{N\pi}$, as was done by Zoller [20]. The only difference between our treatment and that in Ref. [20] is that we follow the conventional normalization so that the coupling constant $g_{\pi NN}$ has its standard value at the pole:

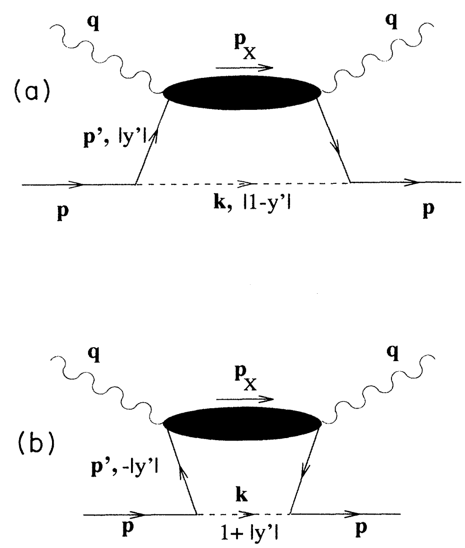


FIG. 3. Time-ordered diagrams for nucleons moving (a) forwards and (b) backwards in time.

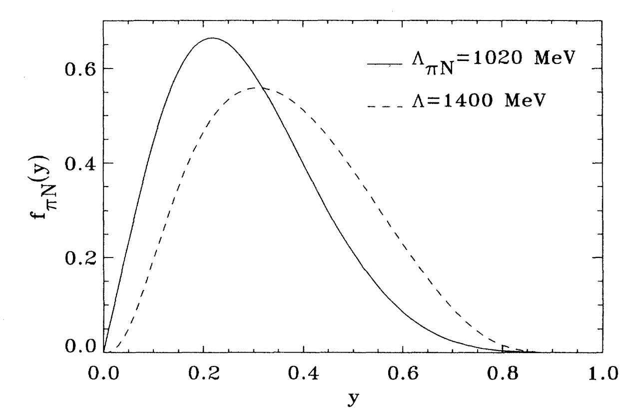


FIG. 4. $\pi N$ distribution function for a dipole form factor and that given in Eq. (17). The cutoffs are chosen so that $\langle n\rangle_{\pi N}\simeq 0.25$ in both cases.

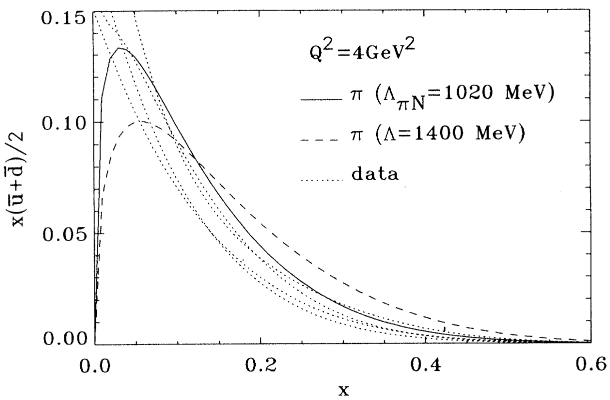


FIG. 5. Proton SU(2) antiquark distributions from DIS on the $\pi N$ component of the nucleon, evaluated for the different $\pi N$ form factors, as in Fig. 4. The data (dotted curves) are the parametrizations of Owens, Morfin and Tung, Eichten *et al.*, and Diemoz *et al.* [38].

$$\mathcal{F}_{N\pi}(k_T^2,y')=\exp\left[\frac{m_N^2-s_{N\pi}}{\Lambda^2}\right] . \tag{16}$$

Within this approach there is an explicit symmetry between the processes in which the intermediate pion and the intermediate nucleon are struck, provided we take the form factor in $f_{\pi N}$ as

$$\mathcal{F}_{\pi N}(k_T^2,y)=\mathcal{F}_{N\pi}(k_T^2,1-y) . \tag{17}$$

Then as long as the same mass parameter $\Lambda$ is used in both vertex functions, Eq. (2) is automatically satisfied.

In Fig. 4 we compare $f_{\pi N}(y)$ with a dipole form factor and with the form factor in Eq. (17). In order to make the comparison meaningful the cutoffs have been chosen to yield the same value of $\langle n\rangle_{\pi N}(\simeq 0.25)$. With the $y$-dependent form factor in Eq. (17) $f_{\pi N}(y)$ is a little broader and peaks at around $y=0.3$, compared with $y\simeq 0.2$ for the covariant formulation with a dipole form factor. Consequently, the convolution of $f_{\pi N}(y)$ with $F_{2\pi}$ for the $y$-dependent form factor will have a slightly smaller peak and extend to marginally larger $x$. This is evident in Fig. 5, where we show the calculated SU(2) antiquark contribution to $\delta^{(\pi N)}F_{2p}(x)$, compared with some recent empirical data at $Q^2=4$ GeV$^2$.

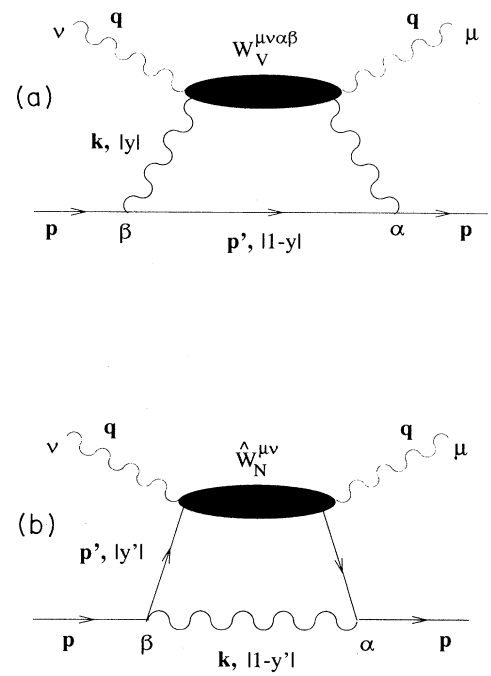


FIG. 6. Time-ordered diagrams for the DIS from (a) vector mesons and (b) nucleons with recoil vector mesons, that are nonzero in the IMF.

## III. VECTOR MESON CONTENT OF THE NUCLEON

In this section we extend the convolution model analysis to the vector-meson sector. Our approach is similar to that described in Sec. II B, namely we use time-ordered perturbation theory to evaluate those diagrams which are nonzero in the IMF. Previous calculations [18,19] of the vector-meson contributions were made in a covariant framework, but with the assumption that the vector-meson and nucleon intermediate states were on-mass-shell. In our approach we self-consistently calculate both the contribution from a struck vector meson [Fig. 6(a)] and from a struck nucleon with a vector-meson recoil [Fig. 6(b)], and show explicitly that the distribution functions for these obey the relation in Eq. (2) exactly.

Starting from the effective $VNN$ interaction (see, e.g., Ref. [2]), where $V=\rho$ or $\omega$, we write in full the vector-meson contribution (with a nucleon recoil) to the nucleon hadronic tensor:

$$\delta^{(VN)}W^{\mu\nu}(p,q)=c_V\int\frac{d^3\mathbf{k}}{(2\pi)^3(2p_0')(2k_0)^2}\left[g_{VNN}^2A_{\alpha\beta}+\frac{f_{VNN}^2}{(4m_N)^2}B_{\alpha\beta}+g_{VNN}\frac{f_{VNN}}{4m_N}C_{\alpha\beta}\right]\frac{\mathcal{F}_{VN}^2(k_T^2,y)}{(p_0-p_0'-k_0)^2}W_V^{\mu\nu\alpha\beta}(k,q) , \tag{18}$$

where

$$\begin{aligned}
A_{\alpha\beta}&=2(m_N^2-p\cdot p')g_{\alpha\beta}+2p_\alpha p'_\beta+2p'_\alpha p_\beta ,\\
B_{\alpha\beta}&=\tfrac{1}{2}[(m_V^2m_N^2-2p\cdot k\,p'\cdot k+m_V^2p\cdot p')g_{\alpha\beta}-(m_N^2+p\cdot p')k_\alpha k_\beta\\
&\quad -m_V^2(p_\alpha p'_\beta+p_\beta p'_\alpha)+p'\cdot k(p_\alpha k_\beta+p_\beta k_\alpha)+p\cdot k(p'_\alpha k_\beta+p'_\beta k_\alpha)] ,\\
C_{\alpha\beta}&=2(p\cdot k-p'\cdot k)g_{\alpha\beta}-(p_\alpha k_\beta+p_\beta k_\alpha)+(p'_\alpha k_\beta+p'_\beta k_\alpha)
\end{aligned} \tag{19}$$

are the $VNN$ vertex trace factors for the vector, tensor, and vector-tensor interference couplings, respectively. The isospin factor $c_V$ is equal to 3 and 1 for isovector and isoscalar mesons, respectively. For an on-mass-shell vector meson, the spin-1 tensor $W^{\mu\nu\alpha\beta}$, symmetric under the interchange of $\mu\leftrightarrow\nu$ and $\alpha\leftrightarrow\beta$, is given by

$$W_V^{\mu\nu\alpha\beta}(k,q)=[\tilde{g}^{\mu\nu}W_{1V}(k,q)+\tilde{k}^{\mu}\tilde{k}^{\nu}W_{2V}(k,q)]\tilde{g}^{\alpha\beta}\ . \tag{20}$$

This form guarantees that the vector current is conserved, $k_{\alpha,\beta}W^{\mu\nu\alpha\beta}=0=q_{\mu,\nu}W^{\mu\nu\alpha\beta}$. Furthermore, it reproduces the correct unpolarized on-shell spin-1 tensor when contracted with the meson polarization vectors ($\epsilon_{\alpha,\beta}$) and summed over the $V$ helicity, $\lambda$ [33]:

$$\begin{aligned}W_V^{\mu\nu}(k,q)=\sum_{\lambda}\epsilon_\alpha^*(\lambda,k)\epsilon_\beta(\lambda,k)W_V^{\mu\nu\alpha\beta}(k,q)=&\left[-g_{\alpha\beta}+\frac{k_\alpha k_\beta}{k^2}\right]W_V^{\mu\nu\alpha\beta}(k,q)\\ &\propto\tilde{g}^{\mu\nu}W_{1V}(k,q)+\tilde{k}^{\mu}\tilde{k}^{\nu}W_{2V}(k,q)\ .\end{aligned} \tag{21}$$

In the case of DIS from a vector particle emitted by a nucleon, Fig. 6(a), contracting the spin-1 tensor $W^{\mu\nu\alpha\beta}$ with the $VNN$ vertex trace factors in Eq. (19), and equating coefficients of $\tilde{g}^{\mu\nu}$ gives

$$\begin{aligned}\delta^{(VN)}W_{1N}(p,q)=c_V\int\frac{d^3\mathbf{k}}{(2\pi)^3(2p_0')(2k_0)^2}&\left\{g_{VNN}^2\left[-6m_N^2+\frac{4p\cdot k\,p'\cdot k}{m_V^2}+2p\cdot p'\right]-\frac{f_{VNN}^2}{2}\left[-3m_V^2+\frac{4p\cdot k\,p'\cdot k}{m_N^2}-\frac{m_V^2p\cdot p'}{m_N^2}\right]\right.\\ &\left.-6g_{VNN}f_{VNN}[p\cdot k-p'\cdot k]\right\}\frac{\mathcal{F}_{VN}^2(k_T^2,y)}{(m_N^2-s_{VN})^2}W_{1V}(k,q)\ .\end{aligned} \tag{22}$$

Using the IMF kinematics (which are similar to those for the $\pi N$ system, except that $m_\pi\rightarrow m_V$), together with the Callan-Gross relation for the nucleon and vector meson, enables the contribution to $F_{2N}$ from vector mesons to be written as a convolution of the vector-meson distribution function $f_{VN}(y)$ with the on-shell vector-meson structure function $F_{2V}(x/y)$, as in Eq. (5), where now

$$\begin{aligned}f_{VN}(y)=\frac{c_V}{16\pi^2}\int_0^\infty dk_T^2&\left\{g_{VNN}^2\left[\frac{[k_T^2+y^2m_N^2+m_V^2][k_T^2+y^2m_N^2+(1-y)^2m_V^2]}{y^2(1-y)m_V^2}+\frac{k_T^2+y^2m_N^2}{1-y}-4m_N^2\right]\right.\\ &+f_{VNN}^2\left[\frac{[k_T^2+y^2m_N^2+m_V^2][k_T^2+y^2m_N^2+(1-y)^2m_V^2]}{2y^2(1-y)m_N^2}-\frac{m_V^2[k_T^2+(2-y)^2m_N^2]}{4(1-y)m_N^2}-m_V^2\right]\\ &\left.+3g_{VNN}f_{VNN}\left[\frac{k_T^2+y^2m_N^2-(1-y)m_V^2}{1-y}\right]\right\}\frac{\mathcal{F}_{VN}^2(k_T^2,y)}{y(1-y)(m_N^2-s_{VN})^2}\ .\end{aligned} \tag{23}$$

The $VNN$ form factor is defined analogously to Eq. (17),

$$\mathcal{F}_{VN}(k_T^2,y)=\exp\left[\frac{m_N^2-s_{VN}}{\Lambda^2}\right]\ , \tag{24}$$

and the $VN$ center-of-mass energy squared is

$$s_{VN}=s_{VN}(k_T^2,y)=\frac{k_T^2+m_V^2}{y}+\frac{k_T^2+m_N^2}{1-y}\ . \tag{25}$$

Suppression of backward moving vector mesons is achieved in the IMF by the energy denominators, as for pions. The vector-meson structure function $F_{2V}$ is not known experimentally, so in our numerical calculations we assume that its $x$ dependence resembles that of the $\pi$ meson structure function, which has been determined experimentally [34].

For the vector-meson recoil process, Fig. 6(b), we evaluate the distribution function $f_{NV}(y')$ using the full spinor structure of $\hat{W}_N^{\mu\nu}$ in Eq. (13):

$$\begin{aligned}\delta^{(NV)}W_{1N}(p,q)=c_V\int\frac{d^3\mathbf{p}'}{(2\pi)^3(2p_0')^2(2k_0)}&\left[g_{VNN}^2A_{\alpha\beta}+\frac{f_{VNN}^2}{(4m_N)^2}B_{\alpha\beta}+g_{VNN}\frac{f_{VNN}}{4m_N}C_{\alpha\beta}\right]\\ &\times\sum_{\lambda}\epsilon_\alpha^*(\lambda,k)\epsilon_\beta(\lambda,k)\frac{\mathcal{F}_{NV}^2(k_T^2,y')}{(p_0-p_0'-k_0)^2}(2m_N\hat{W}_0+2m_N^2\hat{W}_1+2p'\cdot q\hat{W}_2)\ ,\end{aligned} \tag{26}$$

where the tensors $A$, $B$, and $C$ are as in Eq. (19). Performing the contractions over the indices $\alpha,\beta$ leads to the convolution integral of Eq. (6), with the nucleon distribution function with a vector-meson recoil given by

$$f_{NV}(y')=\frac{c_V}{16\pi^2}\int_0^\infty dk_T^2\left\{g_{VNN}^2\left[\frac{[k_T^2+(1-y')^2m_N^2+m_V^2][k_T^2+(1-y')^2m_N^2+y'^2m_V^2]}{y'(1-y')^2m_V^2}+\frac{k_T^2+(1-y')^2m_N^2}{y'}-4m_N^2\right]\right.$$
$$+f_{VNN}^2\left[\frac{[k_T^2+(1-y')^2m_N^2+m_V^2][k_T^2+(1-y')^2m_N^2+y'^2m_V^2]}{2y'(1-y')^2m_N^2}-\frac{m_V^2[k_T^2+(1+y')^2m_N^2]}{4y'm_N^2}-m_V^2\right]$$
$$\left.+3g_{VNN}f_{VNN}\left[\frac{k_T^2+(1-y')^2m_N^2-y'm_V^2}{1-y'}\right]\right\}\frac{\mathcal{F}_{NV}^2(k_T^2,y')}{y'(1-y')(m_N^2-s_{NV})^2}, \quad (27)$$

and where $s_{NV}(k_T^2,y')=s_{VN}(k_T^2,1-y')$. Again, we have evaluated only the diagram with forward moving nucleons which is nonzero in the IMF. It is clear therefore from Eqs. (23) and (27) that the probability distributions for the $VN$ intermediate states are related by $f_{NV}(y')=f_{VN}(1-y')$.

Our numerical results, which are discussed below, rely upon the physical vector-meson–nucleon coupling constants whose values are taken at the poles, as obtained from analyses of $\pi N$ scattering data: $g_{\rho NN}^2/4\pi=0.55, f_{\rho NN}/g_{\rho NN}=6.1$ [35], and $g_{\omega NN}^2/4\pi=8.1, f_{\omega NN}/g_{\omega NN}=0$ [36].

## IV. RESULTS AND DISCUSSION

Figure 7 shows the meson distribution functions $f_{\rho N}$, $f_{\omega N}$, and $f_{\pi N}$ (scaled by a factor $\frac{1}{3}$) for the same vertex cutoff parameter $\Lambda$ ($=1.4$ GeV). The vector-meson component will only be relevant when very hard form factors are employed. To make this point more explicit, we plot in Fig. 8 the average multiplicities $\langle n\rangle_{VN}$ and $\langle n\rangle_{\pi N}$ as a function of $\Lambda$. The dependence on $\Lambda$ is much stronger for the $\rho$ than for $\pi$ mesons. For $\Lambda\lesssim 1.4$ GeV, $\langle n\rangle_{\rho N}$ is considerably smaller than $\langle n\rangle_{\pi N}$, and it is only with much larger cutoffs ($\Lambda\gtrsim 1.8$ GeV) that the $\rho$ multiplicity becomes comparable with that of the $\pi$. Note that $\Lambda=(1000, 1400, 1800)$ MeV corresponds to a dipole $\Lambda_{\pi N}\simeq(650, 1020, 1410)$ MeV for the same $\langle n\rangle_{\pi N}$.

One should observe that the trace factor inside the braces in $f_{VN}(y)$ is divergent in the limit $y\to 0$, so that use of a form factor $\propto\exp[y(m_N^2-s_{VN})]$, which corresponds to a $t$-dependent covariant form factor $\exp[t-m_V^2]$, would make $\delta^{(VN)}F_{2N}(x)$ approach a finite value as $x\to 0$, much like for a perturbative sea distribution. However, there are several problems with accepting such a result, the most obvious of which is that it would violate charge and momentum conservation very badly, since $f_{NV}(y')\to 0$ for $y'\to 1$ and $\to$const as $y'\to 0$ for a form factor $\propto\exp[y'(m_N^2-s_{NV})]$, which in the covariant formalism corresponds to $\exp[t'-m_N^2]$. Furthermore, it would lead to a gross violation of the Adler sum rule, which integrates the flavor combination $u-\bar{u}-d+\bar{d}$, and such a violation has not been observed in the range $1<Q^2<40$ GeV$^2$ [37]. This gives further evidence for the preference of the IMF approach together with the form factor in Eq. (24). Note, however, that because the baryon recoil contributions to the quark and antiquark distributions are related by

$$\delta^{(MB)}u(x)=\delta^{(MB)}\bar{d}(x),$$
$$\delta^{(MB)}d(x)=\delta^{(MB)}\bar{u}(x) \quad (28)$$

the divergent contributions would cancel for the Gottfried (which depends on the combination $u+\bar{u}-d-\bar{d}$) and Gross–Llewellyn-Smith ($u-\bar{u}$

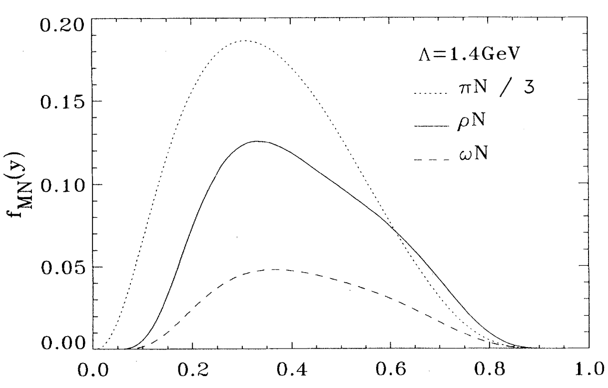


FIG. 7. Meson distribution functions $f_{\rho N}(y)$, $f_{\omega N}(y)$, and $f_{\pi N}(y)$, for $\Lambda=1.4$ GeV. Note the pion distribution is scaled by a factor of $\frac{1}{3}$.

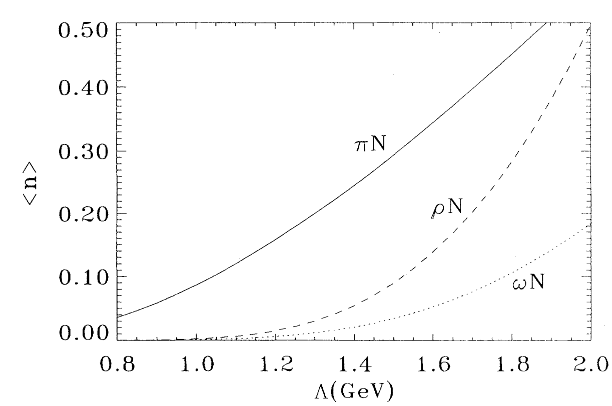


FIG. 8. Average number densities for the $\pi$, $\rho$, and $\omega$ mesons in a nucleon, as a function of the meson-nucleon form factor cutoff.

$+d-\bar{d}$) sum rules.

In previous studies [9,10] restrictions have been obtained on the magnitude of the form factor cutoffs by comparing $\langle y\rangle_{MB}$ with the measured momentum fractions carried by the antiquarks. Even more stringent constraints can be achieved by also demanding that the shape of the meson-exchange contributions to $\bar{q}(x)$,

$$\delta^{(MB)}\bar{q}(x)=\int_x^1 \frac{dy}{y} f_{MB}(y)\bar{q}_M(x/y) , \tag{29}$$

be consistent with the shape of the experimental antiquark distribution [10,16]. Figure 9 shows the calculated antiquark distributions from the $\pi$ component of the nucleon alone and from the pion plus vector-meson structure of the nucleon, for $\Lambda=1.2$ and 1.4 GeV. Clearly the SU(2) $\bar{q}$ content of the nucleon (as parametrized by Owens, Morfin and Tung, Eichten *et al.*, and Diemoz *et al.* [38]) is saturated for $\Lambda\approx 1.2$ GeV in the intermediate-$x$ region. For the $\pi NN$ vertex this corresponds to a dipole form factor cutoff $\Lambda_{\pi N}\approx 830$ MeV—considerably smaller than that used by many authors. We can conclude therefore that for the range of form factor cutoffs allowed by the data, vector mesons play only a marginal role in the DIS process. The maximum value of $\Lambda$ would have to be even smaller with the inclusion of $\pi\Delta$ states in the nucleon, as it has been shown previously [15–18] that these give non-negligible contributions to the nucleon structure function. The $\pi\Delta$ states would also be of relevance to the calculated $\bar{d}-\bar{u}$ difference (and to the Gottfried sum rule) resulting from DIS from the $\pi N$ and $\rho N$ components, which will be partly canceled by this contribution.

At this point we would like to clarify an issue that has been the cause of some confusion recently in the literature. The meson- and baryon-exchange diagrams in Fig. 1 describe physical processes (inclusive baryon and meson leptoproduction) whose cross sections involve physical (renormalized) coupling constants. When integrated over

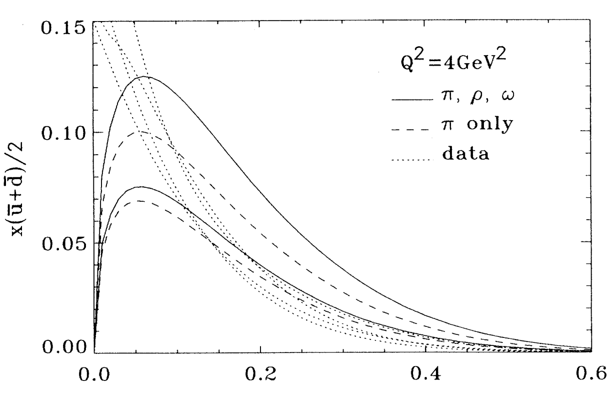


FIG. 9. Proton SU(2) antiquark distributions, calculated with $\pi$ and $\pi+\rho+\omega$ components in the nucleon. The lower (upper) solid and dashed curves correspond to $\Lambda=1.2$ (1.4) GeV. The data are from Ref. [38].

the recoil particles' momenta these yield the inclusive DIS cross sections, which are proportional to the total quark (and antiquark) distributions

$$q(x)=Zq_{\text{bare}}(x)+\sum_{MB}[\delta^{(MB)}q(x)+\delta^{(BM)}q(x)] . \tag{30}$$

Therefore $\delta q(x)$ and the convolution integrals in Eqs. (5), (6), and (29) are expressed in terms of renormalized coupling constants contained in the functions $f(y)$. From Eq. (30) we also determine the bare nucleon probability

$$Z=1-\sum_{MB}\langle n\rangle_{MB} \tag{31}$$

by demanding that the valence number and momentum sum rules are satisfied. We emphasize that all quantities in Eqs. (30) and (31) are evaluated using renormalized coupling constants.

We could, of course, choose to work at a given order in the bare coupling constant, and explicitly verify that the various sum rules are satisfied. For example, to lowest order ($g_0^2$) the total quark distributions would be [39]

$$q(x)=Z\left\{q_{\text{bare}}(x)+\sum_{MB}[\delta^{(MB)}q_{(0)}(x)+\delta^{(BM)}q_{(0)}(x)]\right\} \quad (\text{order } g_0^2) \tag{32}$$

with

$$Z=\left[1+\sum_{MB}\langle n_{(0)}\rangle_{MB}\right]^{-1} \quad (\text{order } g_0^2) , \tag{33}$$

where the subscript (0) indicates that the functions $f(y)$ here are evaluated using bare couplings. Equations (30) and (31) are easily recovered since the bare couplings, to this order, are defined by $g_0^2=g_{\text{ren}}^2/Z$. It would, however, be inconsistent to use Eqs. (32) and (33) with renormalized coupling constants, especially with large form factor cutoffs. As long as the form factors are soft, the difference between the bare and renormalized couplings is quite small. However, with large cutoff masses the bare couplings would need to be substantially bigger than the physical ones. (In fact, the form factor cutoff dependence of the bare $\pi N$ coupling constant in the cloudy bag model [40] showed some 40% difference for very hard form factors—or small bag radii, ~0.6 fm.) In addition, with large values of $\Lambda$, the higher-order diagrams involving more than one meson in the intermediate state would become non-negligible, and the initial assumption that the series in Eq. (1) can be truncated at the one-meson level would be seriously in doubt. Fortunately, we need not consider the multiple-meson contributions, since Fig. 9 clearly demonstrates the difficulty in reconciling the empirical data with quark distributions calculated with such large cutoffs.

Finally, we make some additional comments regarding this justification of our calculation in terms of an incoherent summation of cross sections for the various meson-exchange processes. Because of the pseudoscalar (or pseudovector) nature of the $\pi NN$ vertex, there is no interference between $\pi$ meson and vector-meson exchange. Furthermore, there will be no mixing between the $\omega$ and $\rho$ exchange configurations due to their different isospins. In fact, all of the processes considered in this analysis can be added incoherently. The question remains, however, whether it will be possible to identify an explicit vector-meson contribution to $F_{2N}(x)$ in an unambiguous way in deep-inelastic scattering experiments. While it may be feasible to search for one-pion exchange by observing the distribution of the produced low-momentum baryon spectrum [41], because of the smaller absolute vector-meson cross section it will be difficult to separate this component from both the perturbative background and from that due to other mesons.

## ACKNOWLEDGMENTS

We would like to thank E. M. Henley for his friendly assistance and continued interest in this problem, as well as S. D. Bass, C. A. Hurst, W.-Y. P. Hwang, N. N. Nikolaev, A. W. Schreiber, J. Speth, and V. R. Zoller for useful comments and discussions related to this work. W.M. would like to thank the Institute for Nuclear Theory at the University of Washington for its hospitality during a recent visit, where part of this work was carried out. This work was supported by the Australian Research Council.

---

[1] R. V. Reid, Jr., Ann. Phys. (N.Y.) **50**, 411 (1968); M. M. Nagels, T. A. Rijken, and J. J. de Swart, Phys. Rev. **12**, 744 (1975); M. Lacombe *et al.*, Phys. Rev. D **12**, 1495 (1975); A. J. Jackson, D. O. Riska, and B. Verwest, Nucl. Phys. **A249**, 397 (1975); G. E. Brown and A. D. Jackson, *The Nucleon-Nucleon Interaction* (North-Holland, Amsterdam, 1976).

[2] R. Machleidt, K. Holinde, and Ch. Elster, Phys. Rep. **149**, 1 (1987).

[3] S. Deister, M. F. Gari, W. Krumpelmann, and M. Mahlke, Few Body Systems **10**, 1 (1991); M. Gari and W. Krumpelmann, Z. Phys. A **322**, 689 (1985).

[4] A. W. Thomas and K. Holinde, Phys. Rev. Lett. **63**, 2025 (1989); K. Holinde and A. W. Thomas, Phys. Rev. C **42**, R1195 (1990).

[5] M. T. Jeong and Il-T. Cheon, Phys. Rev. D **43**, 3725 (1991).

[6] A. W. Thomas, Adv. Nucl. Phys. **13**, 1 (1984); R. F. Alvarez-Estrada and A. W. Thomas, J. Phys. G **9**, 161 (1983).

[7] U. G. Meissner, N. Kaiser, and W. Weise, Nucl. Phys. **A466**, 685 (1987); C. Schuren, E. Ruiz Arriola, and K. Goeke, Phys. Lett. B **287**, 283 (1992).

[8] J. D. Sullivan, Phys. Rev. D **5**, 1732 (1972); M. Lusignoli and Y. Srivastava, Nucl. Phys. **B138**, 151 (1978); G. G. Arakelyan, K. G. Boreskov, and A. B. Kaidalov, Yad. Fiz. **33**, 471 (1981) [Sov. J. Nucl. Phys. **33**, 247 (1981)].

[9] A. W. Thomas, Phys. Lett. **126B**, 97 (1983).

[10] L. L. Frankfurt, L. Mankiewicz, and M. I. Strikman, Z. Phys. A **334**, 343 (1989).

[11] A. S. Ito *et al.*, Phys. Rev. D **23**, 604 (1981); M. Ericson and A. W. Thomas, Phys. Lett. **148B**, 191 (1984); G. G. Arakelyan and K. G. Boreskov, Yad. Fiz. **41**, 416 (1985) [Sov. J. Nucl. Phys. **41**, 267 (1985)].

[12] K. Gottfried, Phys. Rev. Lett. **18**, 1174 (1967).

[13] New Muon Collaboration, P. Amaudruz *et al.*, Phys. Rev. Lett. **66**, 2712 (1991).

[14] E. M. Henley and G. A. Miller, Phys. Lett. B **251**, 497 (1990).

[15] A. I. Signal, A. W. Schreiber, and A. W. Thomas, Mod. Phys. Lett. A **6**, 271 (1991).

[16] S. Kumano, Phys. Rev. D **43**, 59 (1991); S. Kumano and J. T. Londergan, *ibid.* **44**, 717 (1991).

[17] W. Melnitchouk, A. W. Thomas, and A. I. Signal, Z. Phys. A **340**, 85 (1991).

[18] W.-Y. P. Hwang, J. Speth, and G. E. Brown, Z. Phys. A **339**, 383 (1991).

[19] A. Szczurek and J. Speth, Jülich Report No. KFA-IKP(TH)-1992-1 (unpublished).

[20] V. Zoller, Z. Phys. C **53**, 443 (1992).

[21] V. Dmitrašinović and R. Tegen, Phys. Rev. C **46**, 1108 (1992).

[22] P. J. Mulders, A. W. Schreiber, and H. Meyer, Nucl. Phys. **A549**, 498 (1992).

[23] E. L. Berger, F. Coester, and R. B. Wiringa, Phys. Rev. D **29**, 398 (1984).

[24] V. M. Belayev and B. L. Ioffe, Nucl. Phys. **B310**, 548 (1988).

[25] R. L. Jaffe, in *Relativistic Dynamics and Quark-Nuclear Physics,* Proceedings of the Workshop, Los Alamos, New Mexico, 1985, edited by M. B. Johnson and A. Pickleseimer (Wiley, New York, 1985).

[26] For scalar mesons, the trace factor in $f_{N\sigma}(y')$ for the structure $\not{q}/2'\cdot q$ is $4m_N^2-m_\sigma^2+(m_N^2-t')(1-y')/y'$, which is clearly related to the trace in $f_{\sigma N}(y)$, namely, $-t+4m_N^2$ when written in terms of the transverse momentum squared (with $m_\pi \to m_\sigma$), and which thereby satisfies Eq. (2), apart from the form factor. For an operator $I/(2m_N)$ the trace factor in $f_{N\sigma}(y')$ is $2t'+2m_N^2-m_\sigma^2$, but this not only violates baryon-number conservation, it also leads to an unphysical (negative) cross section. Similar problems appear in $f_{NV}(y')$ with such an operator.

[27] A. W. Schreiber, W. Melnitchouk, and A. W. Thomas (in preparation).

[28] A. Bodek and J. L. Ritchie, Phys. Rev. D **23**, 1070 (1981); G. Dunne and A. W. Thomas, *ibid.* **33**, 2061 (1986).

[29] L. Heller and A. W. Thomas, Phys. Rev. C **41**, 2756 (1990); M. B. Johnson and J. Speth, Nucl. Phys. **A470**, 488 (1987); L. Kisslinger and M. B. Johnson, Phys. Rev. C **36**, 1081 (1987).

[30] F. Güttner, G. Chanfray, H. J. Pirner, and B. Povh, Nucl. Phys. **A249**, 389 (1984).

[31] S. Weinberg, Phys. Rev. **150**, 1313 (1966).

[32] S. D. Drell, D. J. Levy, and T. M. Yan, Phys. Rev. D **1**, 1035 (1970).

[33] T. Uematsu and T. F. Walsh, Nucl. Phys. **B199**, 93 (1982); P. Hoodbhoy, R. L. Jaffe, and A. Manohar, *ibid.* **B312**, 571 (1989); F. E. Close and S. Kumano, Phys. Rev. D **42**, 2377 (1990).

[34] NA10 Collaboration, B. Betev *et al.*, Z. Phys. C **28**, 15 (1985).

[35] G. Hohler and E. Pietarinen, Nucl. Phys. **B95**, 210 (1975).

[36] W. Grein and P. Kroll, Nucl. Phys. **A338**, 332 (1980).

[37] BEBC Collaboration, D. Allasia *et al.*, Z. Phys. C **28**, 321 (1985).

[38] J. F. Owens, Phys. Lett. B **266**, 126 (1991); J. G. Morfin

and W. K. Tung, Z. Phys. C **52**, 13 (1991); E. Eichten, I. Hinchliffe, K. Lane, and C. Quigg, Rev. Mod. Phys. **56**, 579 (1984); M. Diemoz, F. Ferroni, E. Longo, and G. Martinelli, Z. Phys. C **39**, 21 (1988).

[39] A. W. Schreiber, P. J. Mulders, A. I. Signal, and A. W. Thomas, Phys. Rev. D **45**, 3069 (1992).

[40] S. Théberge, G. A. Miller, and A. W. Thomas, Can. J. Phys. **60**, 59 (1982).

[41] W. Melnitchouk and A. W. Thomas (in preparation).